Applied Computer Systems
ISSN 2255-8691 (online)
ISSN 2255-8683 (print)
2025, vol. 30, no. 1, pp. 68–74
https://doi.org/10.2478/acss-2025-0008
https://content.sciendo.com

VeinKAN: A Finger Vein Recognition Model Based on Kolmogorov–Arnold Networks

An Cong Tran[1*], Nghi Cong Tran[2]
[1–2]*College of Information and Communication Technology, Can Tho University, Can Tho, Vietnam*

Abstract **– Finger vein recognition has become a secure biometric method known for its robustness against spoofing and environmental variations. Traditional methods, which often rely on Multi-layer Perceptrons (MLPs), face limitations in adaptability stemming from fixed activation functions and linear weight constraints. Kolmogorov–Arnold Networks (KANs) offer a novel architecture that enhances nonlinear learning capabilities to improve performance without significantly increasing computational overhead. This study proposes a KAN-based approach for finger vein recognition and evaluates its performance against established Convolutional Neural Network (CNN) models, including InceptionV3, EfficientNet, and MobileNetV3. Experiments on the FV_USM and SDUMLA-HMT benchmark datasets reveal that the proposed model achieves accuracies of 99.3 % and 96.2 %, respectively, surpassing conventional architectures. Despite a higher parameter count (34.81 million), the proposed model maintains an inference time of 1.0096 ms, which is comparable to InceptionV3 (1.006 ms) and notably faster than EfficientNet_B4 (1.349 ms). With a computational complexity of 539.12 MMAC, it supports the feasibility of biometric systems requiring high accuracy and efficient processing. These findings highlight KANs as a promising advancement in biometric recognition technologies.**

Keywords **– CNN, finger vein recognition, Kolmogorov-Arnold networks.**

I. Introduction

In recent years, biometric recognition has become an important area of research, particularly in security and authentication applications. Among the various biometric methods, finger vein recognition has gained significant attention due to its high level of security and resistance to spoofing [1]. Finger veins are unique biometric traits formed by the vascular patterns within the finger (see Fig. 1), making them highly reliable for identification.

Fig. 1. A finger vein image.

Unlike surface-based biometric features, finger vein patterns provide high accuracy and are less influenced by external factors such as dirt or temperature variations.

However, processing and recognising finger vein patterns face several challenges, particularly in extracting complex features and distinguishing between different vein patterns. Numerous methods have been proposed to address these challenges, including traditional machine learning techniques and deep learning approaches.

Traditional machine learning methods, such as Support Vector Machines (SVM), k-Nearest Neighbours (kNN), and statistical feature-based classifiers, have been widely used in finger vein recognition because of their simplicity and effectiveness with structured data. These techniques typically depend on handcrafted features representing vein patterns, including Local Binary Patterns (LBP), Histogram of Oriented Gradients (HOG), and Gabor filters. For instance, Fronitasari and Gunawan utilised LBP with SVM to achieve an accuracy of 92.5 % on a small dataset of 50 subjects [2]. Their approach leveraged LBP's ability to capture local texture details with low computational overhead. However, it struggled with scalability and generalization to larger and more diverse datasets due to its reliance on manually tuned parameters.

Similarly, Ponnusa et al. applied LBP in conjunction with kNN, reporting an equal error rate (EER) of 1.8 % on a proprietary dataset [3]. This method benefited from its robustness to noise, though its performance degraded with low-resolution images. Wang et al. also explored LBP using statistical classifiers, achieving an accuracy of 90.3 % on a dataset of 100 individuals [4]. While this demonstrated computational efficiency, it highlighted limitations in distinguishing subtle vein patterns under varying imaging conditions.

In parallel, HOG-based methods have been investigated for their gradient-based feature extraction capabilities. Zhang and Wang [5] combined HOG with SVM, attaining an accuracy of 94.6 % on the SDUMLA-HMT dataset and leveraging HOG's strength in encoding edge information. However, this approach was less effective against rotational variations and required extensive preprocessing. Kuang et al. extended HOG with a hybrid classifier, achieving a recognition rate of 93.8 % on a custom dataset [6]. This enhancement improved resilience to illumination changes, but it also increased computational complexity.

[*] Corresponding author's e-mail: tcan@ctu.edu.vn
Article received 2025-03-04; accepted 2025-05-06

Additionally, Gabor filters have been widely adopted for their ability to model frequency and orientation in vein images. Ma et al. [7] employed Gabor filters with SVM, reporting an accuracy of 95.2 % on the FV_USM dataset. They benefited from enhanced feature representation of vein orientations, but the sensitivity of the method to parameter tuning limited its adaptability across datasets. Yang et al. [8] integrated Gabor filters with statistical classifiers, achieving an EER of 1.2 % on a dataset of 200 subjects, showcasing robustness to noise and misalignment. However, the multi-scale filtering process significantly increased processing time, hindering real-time applicability.

Although traditional machine learning methods offer simplicity and ease of implementation, they often struggle with complex and imperfect data, such as noisy or incomplete vein patterns. While handcrafted feature-based methods can enhance recognition accuracy by focusing on specific vein characteristics, their dependence on manually designed features limits their ability to fully capture the intricate and variable nature of finger vein patterns. This limitation becomes particularly evident under different imaging conditions or when training data is insufficient, ultimately compromising overall recognition performance.

In recent years, Convolutional Neural Networks (CNNs) and Multi-Layer Perceptrons (MLPs) have become state-of-the-art methods for finger vein recognition. These methods are notable for their ability to automatically extract hierarchical features directly from raw image data, eliminating the need for manual feature engineering. Several significant studies have utilised advanced CNN architectures to enhance recognition accuracy. For example, Krizhevsky et al. [9] introduced AlexNet, a pioneering deep CNN that, when adapted for vein recognition tasks, achieved an accuracy of 96.5 % on a custom dataset of 500 subjects. This success leverages the deep convolutional layers to capture intricate vein patterns. However, the high computational cost (over 700 million FLOPs) and susceptibility to overfitting on smaller datasets posed considerable challenges.

Similarly, Simonyan and Zisserman [10] proposed the VGG architecture that, when fine-tuned for finger vein recognition, reached an accuracy of 97.2 % on the FV_USM dataset. The VGG architecture benefited from its uniform deep structure and robust feature extraction. However, its large parameter count of 138 million made it resource-intensive and impractical for real-time deployment on constrained devices.

Subsequent research leveraging architectures like ResNet and DenseNet has further improved performance by addressing gradient vanishing issues and enhancing feature reuse. However, the specific results for vein recognition varied depending on the dataset size and the preprocessing techniques used.

To address the challenges associated with limited training data, some researchers have employed Generative Adversarial Networks (GANs) to augment datasets with synthetic vein samples. Goodfellow et al. introduced the foundational GAN framework [11], which Yang et al. adapted for finger vein recognition [12]. This adaptation led to the generation of synthetic images that improved model accuracy from 92.3 % to 95.8 % on the SDUMLA-HMT dataset. This approach effectively enriched training diversity and reduced the risk of overfitting. However, the quality of the synthetic samples was inconsistent, and occasionally introduced artefacts that negatively impacted performance on real-world data.

In addition to GANs, researchers also used transfer learning. Yosinski et al. [13] demonstrated that pre-trained models on large-scale datasets like ImageNet could be fine-tuned for finger vein recognition, achieving an accuracy of 96.8 % on a dataset of 300 subjects while reducing training time by 20 % compared to training from scratch. This method capitalized on pre-learned features to enhance generalization, although its effectiveness decreased when vein-specific patterns deviated significantly from the natural image domain of ImageNet. These advancements highlight the superior feature-learning capabilities of deep learning compared to traditional methods. However, they also reveal ongoing trade-offs between accuracy, computational efficiency, and adaptability to small or specialized datasets.

CNNs and MLPs have demonstrated their effectiveness in handling complex image data, such as finger vein patterns. However, these architectures also have limitations, such as the sensitivity to overfitting when the training dataset lacks diversity. Additionally, they rely on fixed activation functions and linear weights, which may restrict their adaptability to highly variable and intricate vein structures. Several factors, such as skin texture, lighting conditions, and individual physiological differences can influence the complexity of these structures. Therefore, there is a need for more advanced deep learning architectures that can enhance representational power and adaptability to create more accurate and efficient finger vein recognition solutions.

To address the limitations of CNNs and MLPs, such as their dependence on fixed activation functions and potential inefficiencies with highly nonlinear or high-dimensional data, Kolmogorov–Arnold Networks (KANs) have emerged as a promising alternative. KANs are based on the Kolmogorov–Arnold theorem [14]–[15], which states that any continuous multivariate function can be expressed as a composition of univariate functions. This provides a solid theoretical foundation for modelling complex relationships.

Liu et al. [16] have recently introduced KANs as a neural architecture that can dynamically learn activation functions tailored to specific data, moving away from predefined functions like ReLU or sigmoid. This flexibility allows KANs to operate without the constraints of linear weight assignments. In their experiments with synthetic high-dimensional datasets, the authors reported that KANs achieved a mean squared error (MSE) of 0.012, outperforming CNNs, which had an MSE of 0.045 by adapting more effectively to nonlinear patterns. This adaptability positions KANs as a powerful tool for approximating complex functions and processing multidimensional data, such as the intricate vascular patterns in finger vein images.

Recent studies have demonstrated the potential of KANs across various domains, particularly in tasks that require high accuracy in nonlinear function approximation and pattern recognition. For instance, Wang et al. applied KANs to CEST MRI data analysis, achieving higher accuracy in extrapolating fitting metrics [17]. Their validation loss was 15 % lower than that of Multi-Layer Perceptrons (MLPs) based on a dataset of brain scans from 12 healthy volunteers. This method outperformed traditional multi-pool Lorentzian fitting by capturing subtle chemical exchange patterns more effectively. However, it necessitated significant preprocessing, which increased computational overhead by 20 %.

Similarly, Huang et al. [18] employed Kolmogorov–Arnold Networks (KANs) for bio-signal classification, achieving an area under the ROC curve (AUC) of 0.95, compared to 0.90 for convolutional neural networks (CNNs). This finding demonstrates KANs' effectiveness in pattern recognition, which may also apply to retinal images. Furthermore, Li et al. [19] investigated KANs as a backbone for medical image enhancement. They achieved a 10 % improvement in peak signal-to-noise ratio (PSNR) compared to CNN-based methods on the generated medical images. This research highlights the ability of KANs to enhance fine-grained features, albeit with a processing speed trade-off, being approximately 1.5 times slower than CNN baselines due to their computational demands.

Collectively, these studies underscore KANs' efficacy in handling complex, high-dimensional data and nonlinear patterns, offering a compelling foundation for their application in finger vein recognition, where adaptability and precision are paramount. However, challenges in computational efficiency and resource demands warrant further investigation.

These findings highlight the potential of Kolmogorov–Arnold Networks in medical image processing, spanning classification, segmentation, and image reconstruction. Therefore, in this study, we propose a finger vein recognition method based on KANs, named VeinKAN. This approach is designed to enhance the feature extraction and classification of finger vein patterns and evaluate the performance of KANs compared to CNN and MLP architectures.

The remainder of this paper is organized as follows. Section 2 introduces the proposed method, describing Kolmogorov–Arnold Networks (KANs) and their application in finger vein recognition. Section 3 presents the experimental results, including performance comparisons between KANs and traditional deep learning models such as CNNs and MLPs. Finally, Section 4 concludes the study by summarising the key findings and discussing potential future research directions.

II. METHODOLOGY

A. Kolmogorov–Arnold Networks

Kolmogorov–Arnold Network (KAN) is a mathematical model based on the Kolmogorov–Arnold theorem, developed from the research of mathematicians Andrey Kolmogorov and Vladimir Arnold. The Kolmogorov–Arnold theorem states that any continuous function of multiple variables can be represented as a combination of univariate functions and addition operations [14], [15]. This property makes KANs a powerful tool for approximating complex functions and processing multidimensional data.

The Kolmogorov–Arnold theorem allows for the representation of a function $f(x_1, x_2,\ldots, x_n)$ of n variables in the form of (1):

$$f(x) = \sum_{q=1}^{2n+1} \phi_q \left(\sum_{p=1}^{n} \phi_{q,p}(x_p) \right). \tag{1}$$

In the Kolmogorov–Arnold representation, the functions ϕ_q and $\phi_{q,p}$ are univariate functions, which enables KANs to efficiently approximate complex functions by combining simpler functions. This capability is particularly advantageous in high-dimensional and nonlinear data processing tasks, such as image recognition and signal processing.

Unlike traditional neural networks such as Multi-Layer Perceptrons (MLPs), which rely on fixed activation functions (e.g., ReLU), KANs introduce learnable activation operators on the edges of the network. This allows KANs to decouple nonlinear transformations from standard weight structures, thereby enhancing the expressive power and flexibility of the network. The architecture of a Kolmogorov–Arnold Network is illustrated in Fig. 2.

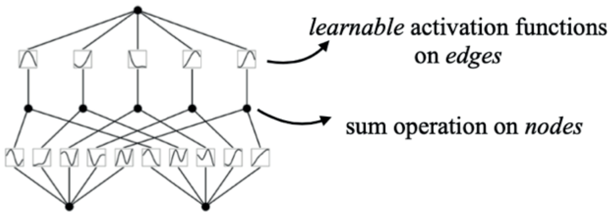

Fig. 2. Kolmogorov–Arnold Network architecture [16].

Advantages of Kolmogorov–Arnold Networks:

- Capability for complex function approximation: KANs can approximate nonlinear and high-dimensional functions with high accuracy. This makes them well-suited for processing complex data, such as finger vein images, where intricate patterns must be effectively captured.
- Computational efficiency: Compared to traditional deep learning models like CNNs, KANs often require fewer parameters and can reduce computational time. This is particularly beneficial for real-time processing applications where efficiency is crucial.
- Robustness to noisy data: KANs can process incomplete or noisy data, an essential feature in biometric recognition. In real-world scenarios, finger vein images can be affected by noise, lighting variations, or motion blur, yet KANs maintain high accuracy due to their adaptive activation mechanisms.

The deep architecture of Kolmogorov–Arnold Networks (deep KANs) is designed to maximize their ability to approximate complex functions. This architecture consists of multiple layers, where each layer applies nonlinear transformations to the input data. In a deep KAN, multiple stages of Kolmogorov-Arnold expansions are combined to form a hierarchical structure. Specifically, a deep KAN can be represented in (2).

$$\mathrm{KAN}(x) = (\phi_1 \circ \phi_2 \circ \phi_3)(x)\,, \tag{2}$$

where, each ϕ_i is a learnable nonlinear mapping block, x approximating the Kolmogorov–Arnold decomposition. Each block is typically implemented using a set of fully connected sub-modules whose parameters are learned simultaneously with the network. These sub-modules replace standard MLP layers, allowing KANs to learn a set of optimized activation functions that are specifically tailored to the characteristics of the input data. The architecture of a deep KAN is illustrated in Fig. 3.

Finger vein recognition is a complex problem due to the diversity and nonlinear nature of vein patterns. Traditional methods and existing deep learning approaches often struggle to extract and analyse these intricate features effectively. With their capability to approximate complex functions and process high-dimensional data, Kolmogorov–Arnold Networks present a promising solution to address these challenges.

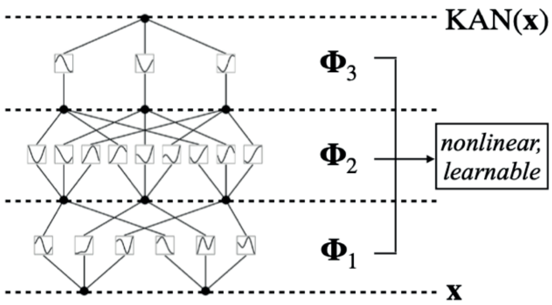

Fig. 3. The architecture of a deep KAN.

B. KAN-Based Finger Vein Recognition Model

In this study, we propose a finger vein classification model, VeinKAN, based on KANs, combined with CNN-based feature extraction techniques, as illustrated in Fig. 4. The model consists of three main stages: ROI extraction, feature extraction, and finger vein classification.

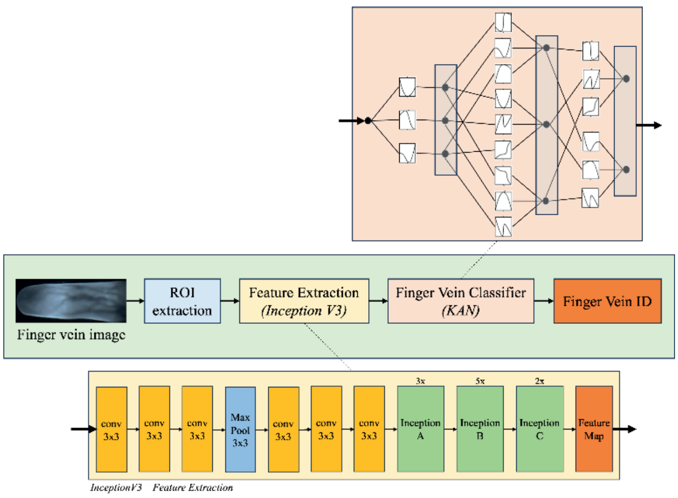

Fig. 4. KAN-based finger vein recognition model.

Before feature extraction, the finger vein image is processed to extract the Region of Interest (ROI). This step aims to eliminate redundant parts of the image and focus on the finger vein region, thereby enhancing the effectiveness of feature extraction. The main steps in this phase include:

- Image preprocessing: The input image is cleaned and normalized to reduce noise and improve quality.
- Vein region identification: Image processing techniques such as edge detection and image segmentation are applied to locate the finger vein region.
- ROI cropping: The image is cropped to retain only the Region of Interest, reducing data size and improving processing speed.

After ROI extraction, the feature extraction stage utilizes the Inception V3 convolutional network. Convolution layers and pooling layers are employed to extract meaningful features from the finger vein images. Specifically, the architecture consists of:

- 3×3 convolution layers to detect local vein features such as edges, contours, and more complex vein structures;
- 3×3 Max Pooling layer to reduce the spatial dimensions of the extracted features;
- Inception blocks to capture multi-scale and more complex vein patterns.

The features extracted in this stage are then passed to the classification phase. The classification phase utilizes KANs to classify the extracted finger vein features. This model employs KANs to categorize the vein characteristics into classes corresponding to different individuals.

C. Model Training and Testing Process

The training and testing process of the proposed finger vein recognition model is illustrated in Fig. 5.

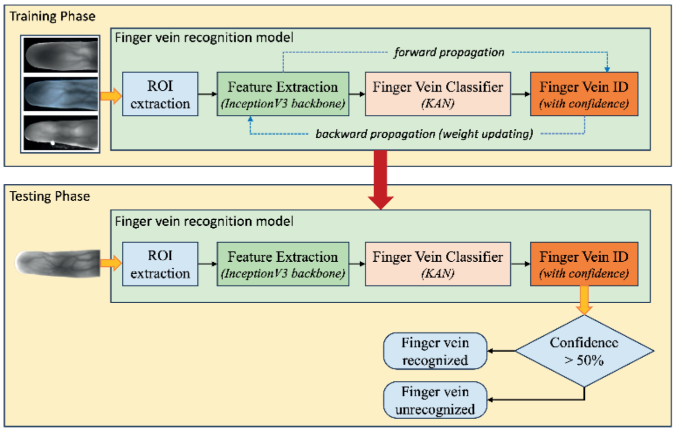

Fig. 5. Finger vein recognition model training and testing process.

The input for the training process consists of a labelled finger vein dataset corresponding to different individuals. The input images undergo preprocessing and ROI extraction before being used for model training. After ROI extraction, finger vein features are extracted using the InceptionV3 convolutional network as the backbone. The extracted features are then fed into the Kolmogorov–Arnold Network for classification. We employ the cross-entropy loss function, defined in (3) as follows:

$$L = -\sum_{i=1}^{N} y_i \log(\hat{y}_i) , \tag{3}$$

where y_i represents the true label, $\hat{y}_i$ represents the predicted probability for each class i, and N is the total number of classes.

The backpropagation step in the training process updates the model weights to minimize errors and improve performance.

The testing and evaluation process consists of the following steps. The finger vein images used for testing first undergo preprocessing and ROI extraction, similar to the training phase. The processed images are then fed into the trained model, which consists of the InceptionV3 backbone and the KAN classification network, to classify the finger vein patterns. The classification result is accompanied by a confidence score, reflecting the model's certainty in its prediction. The input finger vein image is recognized if the confidence score exceeds 50 %. Otherwise, the input image is treated as invalid (unrecognised).

III. EXPERIMENTAL RESULTS

In this section, we present the evaluation results of the proposed model, including a description of the experimental dataset, the metrics used in the experiments, the benchmark models for comparison, the performance results, and an analysis of these findings.

A. Experimental Datasets

We use two finger vein datasets to evaluate the proposed model: FV_USM [20] and SDUMLA-HMT [21]:

- FV_USM: Consists of 491 classes, with 12 images per class, totalling 5904 images. This dataset is relatively well-standardized, with high-quality images.
- SDUMLA-HMT: Consists of 363 classes, with 6 images per class, totalling 3836 images. This dataset presents a higher difficulty level than FV_USM due to the smaller number of images per class. Additionally, the image quality varies more significantly across samples.

A summary of these two datasets is presented in Table I.

TABLE I
EXPERIMENTAL DATASETS

Dataset	No. of classes	No. of images/class	No. of images
FV_USM	491	12	5904
SDUMLA-HMT	636	6	3816

Each dataset is divided into two subsets: one for training the model and the other for testing the model. We allocate 70 % of the images for the training phase and 30% for the testing phase.

B. Experimental Setup

The values of the hyperparameters used in the experiments are as follows:

- Optimizer: The Adam optimizer was employed with an initial learning rate of 10^{-4}.
- Batch size: A batch size of 64 was selected (adjusted to accommodate the memory capacity of the GPU used for model training).
- Loss function: Categorical cross-entropy was adopted as the loss function.
- Number of epochs: An early stopping strategy was implemented if the accuracy did not improve after 10 epochs on the validation dataset. However, to ensure fairness in comparing the experimental results of the proposed model with baseline models, the maximum number of epochs was set to 100.
- Hardware: An NVIDIA RTX 3060 GPU was utilized for both the training and recognition (testing) phases.
- Evaluation metrics: The Top-1 accuracy metric was used to assess the model's accuracy as defined in (4). Additionally, we employed supplementary metrics to evaluate the model's performance, including the number of model parameters, inference time, and MMAC (Million Multiply-Accumulate Operations per Second).

$$\text{Top-1 Accuracy} = \frac{\text{Number of correct predictions}}{\text{Total number of predictions}} \tag{4}$$

The experimental results of the proposed model were compared with those of several state-of-the-art (SOTA) classification models, including Inception V3, EfficientNet_B0, EfficientNet_B4, and MobileNetV3.

C. Experimental Results

Table II presents the Top-1 Accuracy (%) of various deep learning models evaluated on two datasets: FV_USM and SDUMLA-HMT. The proposed VeinKAN model achieves higher accuracy compared to the baseline models.

TABLE II
THE TOP-1 ACCURACY OF THE MODELS ACROSS THE TWO EXPERIMENTAL DATASETS (%)

Model	FV_USM	SDUMLA_HMT
VeinKAN	99.31	96.23
InceptionV3	95.60	93.15
MobileNetV3	91.68	88.76
EfficientNet_BO	93.12	91.41
EfficientNet_B4	92.86	90.86

The results demonstrate that the proposed model achieves the highest accuracy on both datasets, highlighting the superior classification capability of the KANs model, which leverages its ability to learn appropriate activation functions autonomously. Specifically, on the FV_USM dataset, the proposed model attains an accuracy of 99.3 %, surpassing the second-best model (InceptionV3) by 3.7 %. On the SDUMLA-HMT dataset, the proposed model achieves an accuracy of 96.2 %, outperforming InceptionV3 by 3.1 % and MobileNetV3 by 7.5 %. All models exhibit lower accuracy on the SDUMLA-HMT dataset compared to the FV_USM dataset, attributable to the significantly smaller number of samples per class in SDUMLA-HMT (6 samples) compared to FV_USM (12 samples).

Among the compared models, InceptionV3 exhibits the highest performance, followed by EfficientNet_B4 and EfficientNet_B0, while MobileNetV3 demonstrates the lowest accuracy across both datasets. The performance gap between the EfficientNet variants suggests that increasing model depth does not always yield significant improvements for this specific task.

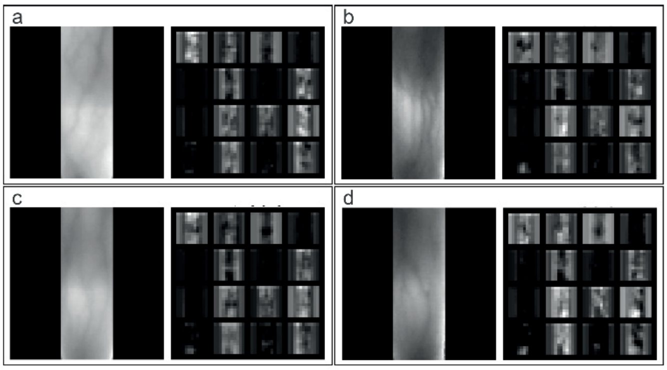

Fig. 6. Finger-vein image sample and extracted feature map.

Figure 6 shows a sample finger-vein image alongside the corresponding feature map extracted by the InceptionV3 backbone. This feature map highlights the unique vascular patterns in the original image. These patterns are subsequently fed into the KAN classifier, which identifies the individual based on their vein characteristics.

Table III compares the models based on three key criteria: the number of parameters (in millions), computational complexity (MMAC), and inference time (in milliseconds). These results enable an evaluation of the trade-offs between accuracy, computational efficiency, and practical deployability of each model. The parameters were computed based on the SDUMLA-HMT dataset.

TABLE III

PERFORMANCE EVALUATION

Model	No. of parameters (millions)	MMAC	Inference time (ms)
VeinKAN	34.81	539.12	1.0096
InceptionV3	23.10	540.00	1.0060
MobileNetV3	4.99	108.85	0.8640
EfficientNet_BO	18.79	425.16	1.3490
EfficientNet_B4	5.18	61.59	0.8340

The proposed model has the highest number of parameters, totalling 34.81 million, which is significantly greater than InceptionV3 (23.1 million parameters) and substantially exceeds EfficientNet_B0 (4.99 million parameters) and MobileNetV3 (5.18 million parameters). This indicates that the proposed model can learn more features, which may account for its superior accuracy on the FV_USM and SDUMLA-HMT datasets. In contrast, EfficientNet_B0 and MobileNetV3, with the lowest parameter counts, are better suited for resource-constrained systems.

In terms of computational complexity, the proposed model exhibits an MMAC value of 539.12, which is comparable to InceptionV3 (540 MMAC) but significantly higher than EfficientNet_B0 (108.85 MMAC) and MobileNetV3 (61.59 MMAC). Meanwhile, EfficientNet_B4 has a computational complexity of 425.16 MMAC, lower than both the proposed model and InceptionV3, yet still demanding more resources than EfficientNet_B0. This suggests that EfficientNet models, particularly the B0 variant, can perform better at a lower computational cost, making them optimal choices for real-time applications with hardware constraints.

Inference time is a critical factor in practical deployment scenarios. MobileNetV3 achieves the lowest inference time (0.834 ms), followed closely by EfficientNet_B0 (0.864 ms). This reflects the efficiency of these lightweight models in rapidly processing input data. In comparison, the proposed model records an inference time of 1.0096 ms, nearly equivalent to InceptionV3 (1.006 ms), and notably faster than EfficientNet_B4 (1.349 ms). Although EfficientNet_B4 offers higher accuracy than EfficientNet_B0 and MobileNetV3, its elevated inference time may pose a limitation for applications requiring rapid processing speeds.

IV. Conclusion

The proposed model achieves the highest accuracy while maintaining a reasonable inference time. MobileNetV3 and EfficientNet_B0 emerge as the most suitable models for real-time applications and resource-constrained systems due to their low parameter counts, reduced computational complexity, and fast inference speeds. Although EfficientNet_B4 delivers strong accuracy, its elevated inference time may render it less suitable for applications requiring rapid inference.

Future research areas could focus on optimising the model to reduce computational complexity while preserving high accuracy. Additionally, techniques such as quantisation, pruning, or dimensionality reduction could be employed to enhance inference performance without significantly compromising model quality.

References

[1] N. Hu, H. Ma, and T. Zhan, "Finger vein biometric verification using block multi-scale uniform local binary pattern features and block two-directional two-dimension principal component analysis," *Optik*, vol. 208, Apr. 2020, Art. no. 163664. https://doi.org/10.1016/j.ijleo.2019.163664

[2] D. Fronitasari and D. Gunawan, "Palm vein recognition by using modified of local binary pattern (LBP) for extraction feature," in *Proceedings of the 15th International Conference on Quality in Research (QiR): International symposium on electrical and computer engineering,* Nusa Dua, Bali, Indonesia, Jul. 2017, pp. 18–22. https://doi.org/10.1109/QIR.2017.8168444

[3] V. Ponnusamy, A. Sridhar, A. Baalaaji, and M. Sangeetha, "A palm vein recognition system based on a support vector machine," *IEIE Transactions on Smart Processing & Computing,* vol. 8, no. 1, Feb. 2019, pp. 1–7. http://doi.org/10.5573/IEIESPC.2019.8.1.001

[4] Y. D. Wang, Q. Y. Yan, and K. F. Li, "Hand vein recognition based on multi-scale LBP and wavelet," in *Proceedings of the 2011 International Conference on Wavelet Analysis and Pattern Recognition*, Guilin, China, Jul. 2011, pp. 214–218. https://doi.org/10.1109/ICWAPR.2011.6014480

[5] X. Zhang, and W. Wang, “Finger vein recognition method based on GLCM-HOG and SVM,” in *Proceedings of the 2020 IEEE 3rd International Conference on Information Systems and Computer Aided Education (ICISCAE)*, Dalian, China, Sep. 2020, pp. 698–701. https://doi.org/10.1109/ICISCAE51034.2020.9236798

[6] H. Kuang, Z. Zhong, X. Liu, and X. Ma, “Palm vein recognition using convolution neural network based on feature fusion with HOG feature,” in *Proceedings of the 5th International Conference on Smart Grid and Electrical Automation (ICSGEA)*, Zhangjiajie, China, Jun. 2020, pp. 295–299. https://doi.org/10.1109/ICSGEA51094.2020.00070

[7] X. Ma, X. Jing, H. Huang, Y. Cui, and J. Mu, “Palm vein recognition scheme based on an adaptive Gabor filter,” *Iet Biometrics*, vol. 6, no. 5, Jan. 2017, pp. 325–333. https://doi.org/10.1049/iet-bmt.2016.0085

[8] J. Yang, Y. Shi, and J. Yang, “Finger-vein recognition based on a bank of Gabor filters,” in *Computer Vision–ACCV 2009: 9th Asian Conference on Computer Vision*, Xi’an, Sep. 2009, Revised Selected Papers, Part I 9, 2010, pp. 374–383. https://doi.org/10.1007/978-3-642-12307-8_35

[9] A. Krizhevsky, I. Sutskever, and G.E. Hinton, “ImageNet classification with deep convolutional neural networks,” *Advances in Neural Information Processing Systems*, vol. 25, 2012, pp. 1097–105. https://proceedings.neurips.cc/paper_files/paper/2012/file/c399862d3b9d6b76c8436e924a68c45b-Paper.pdf

[10] K. Simonyan, and A. Zisserman, “Very deep convolutional networks for large-scale image recognition,” *arXiv preprint arXiv:1409.1556*, Sep. 2014. https://doi.org/10.48550/arXiv.1409.1556

[11] I.J. Goodfellow, J. Pouget-Abadie, M. Mirza, B. Xu, D. Warde-Farley, S. Ozair, A. Courville and Y. Bengio, “Generative adversarial nets,” *Advances in Neural Information Processing Systems*, vol. 27, 2014, pp. 2672–2680. https://proceedings.neurips.cc/paper_files/paper/2014/file/f033ed80deb0234979a61f95710dbe25-Paper.pdf

[12] H. Yang, P. Fang, and Z. Hao, “A GAN-based method for generating finger vein dataset,” in *Proceedings of the 2020 3rd International Conference on Algorithms, Computing and Artificial Intelligence*, Dec. 2020, pp. 1–6. https://doi.org/10.1145/3446132.3446150

[13] J. Yosinski, J. Clune, Y. Bengio, and H. Lipson, “How transferable are features in deep neural networks?” *Advances in Neural Information Processing Systems*, vol. 27, 2014. https://proceedings.neurips.cc/paper_files/paper/2014/file/532a2f85b6977104bc93f8580abbb330-Paper.pdf

[14] A.N. Kolmogorov, “On the representation of continuous functions of several variables by superpositions of continuous functions of a smaller number of variables,” in *American Mathematical Society Translations – Series 2*, vol. 17, 1961, pp. 369–373.

[15] A.N. Kolmogorov, “On the representation of continuous functions of many variables by superposition of continuous functions of one variable and addition,” *American Mathematical Society Translations*, vol. 2, no. 28, 1963, pp. 55–59.

[16] Z. Liu, Y. Wang, S. Vaidya, F. Ruehle, J. Halverson, M. Soljačić, T.Y. Hou, and M. Tegmark, “KAN: Kolmogorov–Arnold networks,” *arXiv preprint arXiv:2404.19756*, Apr. 2024. https://doi.org/10.48550/arXiv.2404.19756

[17] J. Wang, P. Cai, Z. Wang, H. Zhang, and J. Huang, “CEST-KAN: Kolmogorov–Arnold networks for CEST MRI data analysis,” *arXiv preprint arXiv:2406.16026*, Jun. 2024. https://doi.org/10.48550/arXiv.2406.16026

[18] Z. Huang, J. Cui, L. Yu, L.F. Herbozo Contreras, and O. Kavehei, “Abnormality detection in time-series bio-signals using Kolmogorov–Arnold networks for resource-constrained devices,” *medRxiv*, 2024-06, 2024. https://doi.org/10.1101/2024.06.04.24308428

[19] C. Li, X. Liu, W. Li, C. Wang, H. Liu, Y. Liu, Z. Chen, and Y. Yuan, “U-KAN makes strong backbone for medical image segmentation and generation,” in *Proceedings of the AAAI Conference on Artificial Intelligence*, vol. 39, no. 5, Apr. 2025, pp. 4652–4660. https://doi.org/10.1609/aaai.v39i5.32491

[20] M.S.M. Asaari, S.A. Suandi, and B.A. Rosdi, “Fusion of band limited phase only correlation and width centroid contour distance for finger based biometrics,” *Expert Systems with Applications*, vol. 41, no. 7, pp. 3367–3382, Jun. 2014. https://doi.org/10.1016/j.eswa.2013.11.033

[21] Y. Yin, L. Lili, and S. Xiwei, "SDUMLA-HMT: A multimodal biometric database,” in *Biometric Recognition: 6th Chinese Conference*, CCBR 2011, Beijing, China, Dec. 2011. Proceedings 6. Springer Berlin Heidelberg, 2011, pp. 260–268. https://doi.org/10.1007/978-3-642-25449-9_33

An Cong Tran is a Senior Lecturer at the College of Information and Communication Technology at Can Tho University, Vietnam. He received a Master’s degree (Hons) in Computer Science from the Asian Institute of Technology (AIT), Thailand, and a PhD in Computer Science from Massey University, New Zealand. His current research interests include description logic learning, ontology learning, applications of blockchain in the public sector, and applications of deep learning methods.
E-mail: tcan@ctu.edu.vn
ORCID iD: https://orcid.org/0000-0001-6184-909X

Nghi Cong Tran is a Lecturer at the College of Information and Communication Technology at Can Tho University in Can Tho, Vietnam. He earned his PhD from National Central University in Taiwan. His current research focuses on machine learning, deep learning, computer vision, and biometric authentication.
E-mail: tcnghi@ctu.edu.vn
ORCID iD: https://orcid.org/0009-0009-7249-6715